Electronic Supplementary Material (ESI) for Green Chemistry.

Supplementary Information

Valorization of Fast-Growing Paulownia Wood to Green Chemicals and Green Hydrogen

Li Quan Lee, Hu Zhao, Junyu Ge, Yan Zhou and Hong Li

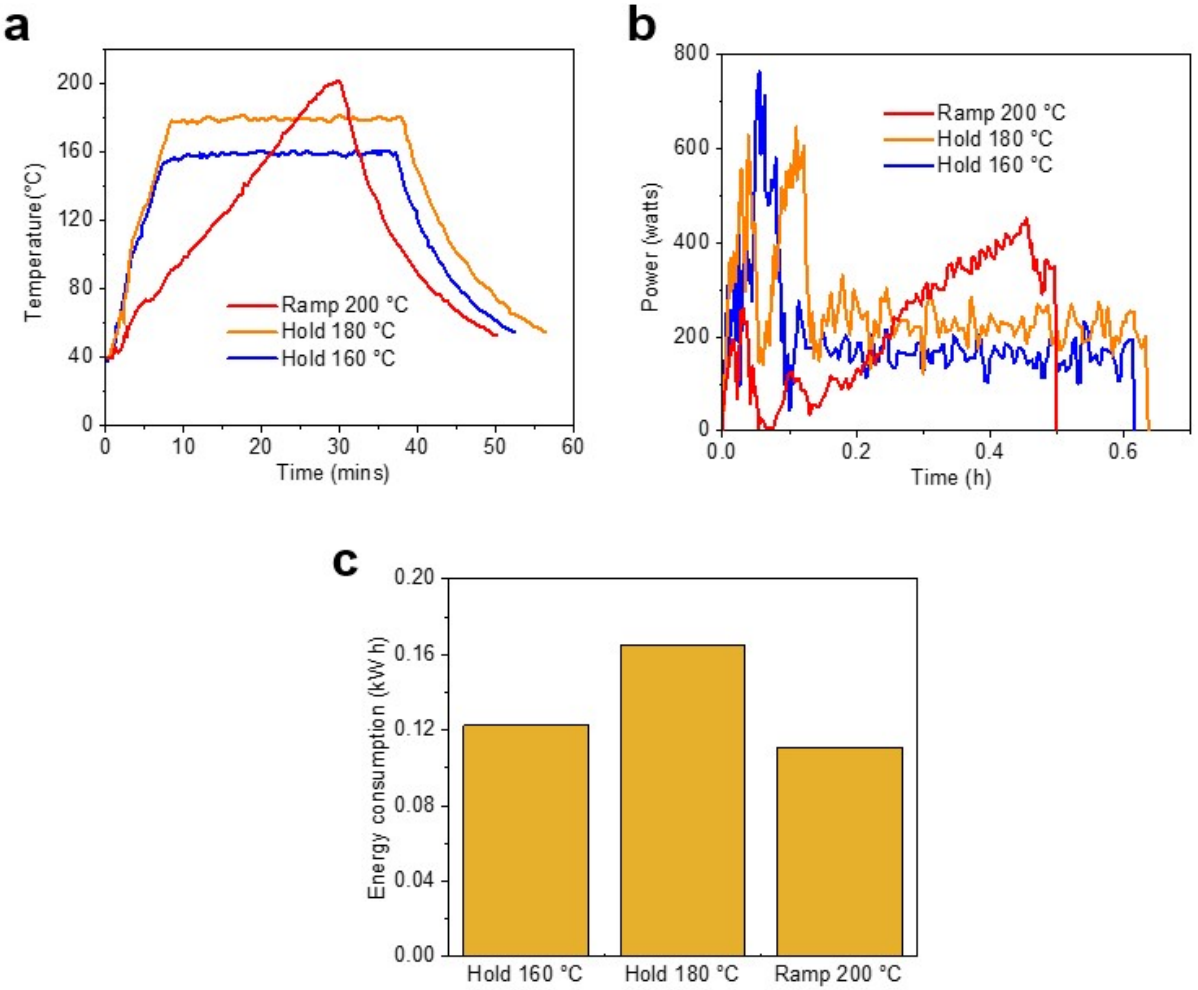

Fig. S1 Microwave heating of 3 settings Ramp 200 °C, Hold 180 °C and 160 °C - a) Temperature profiles; b) Power profiles; and c) Energy consumption comparison.

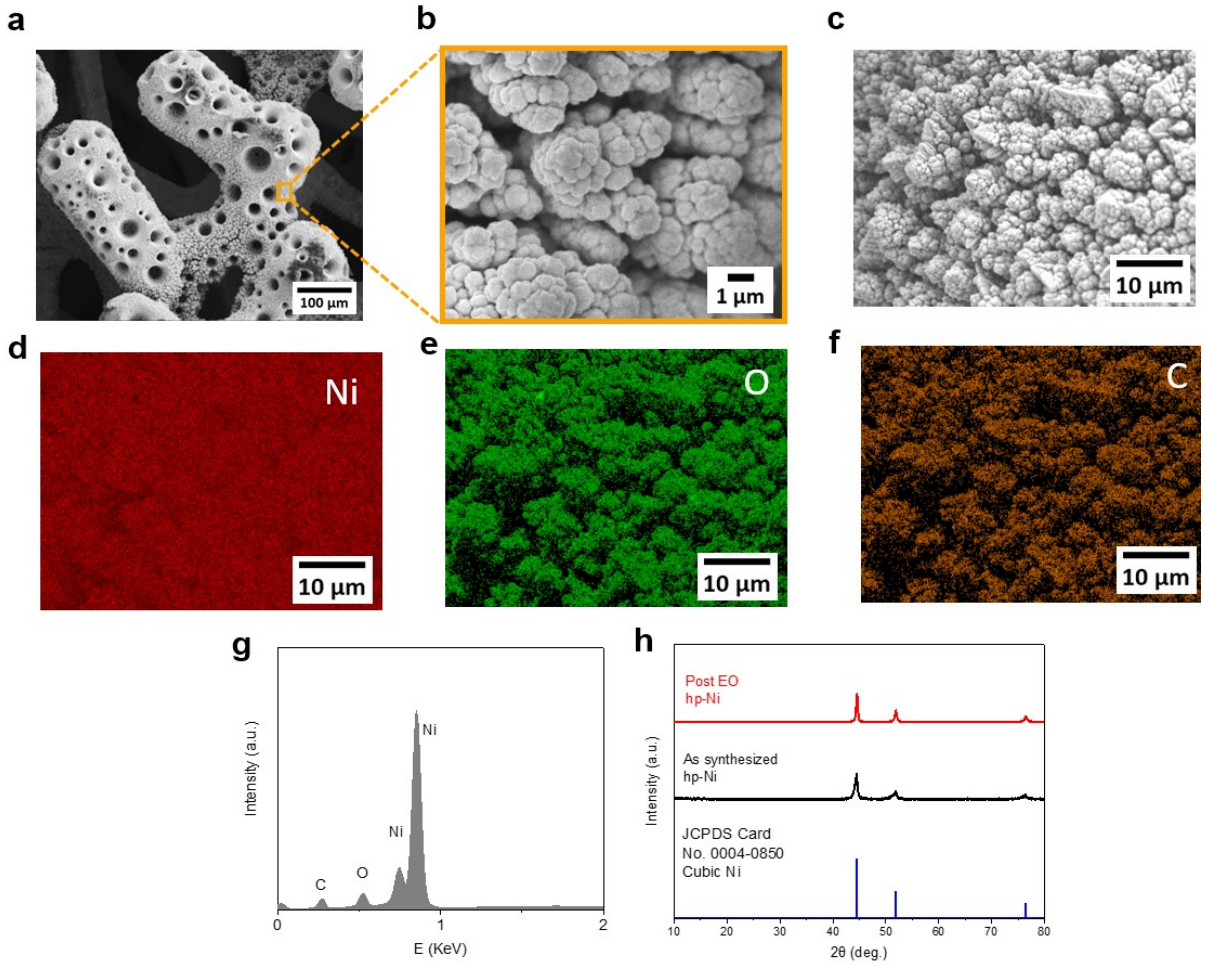

Fig. S2 *hp*-Ni - a) SEM image; b) Magnified image of image (a); *hp*-Ni EDS - c) SEM image used for EDS analysis; d) Nickel element mapping image, e) Oxygen element mapping image, f) Carbon element mapping image, g) EDS spectrum of area in image (c); h) XRD of *hp*-Ni - (red) Post electrooxidation (EO) of HPW, (black) As synthesized ,and (blue) cubic Ni standard from JCPDS card No. 0004-0850.

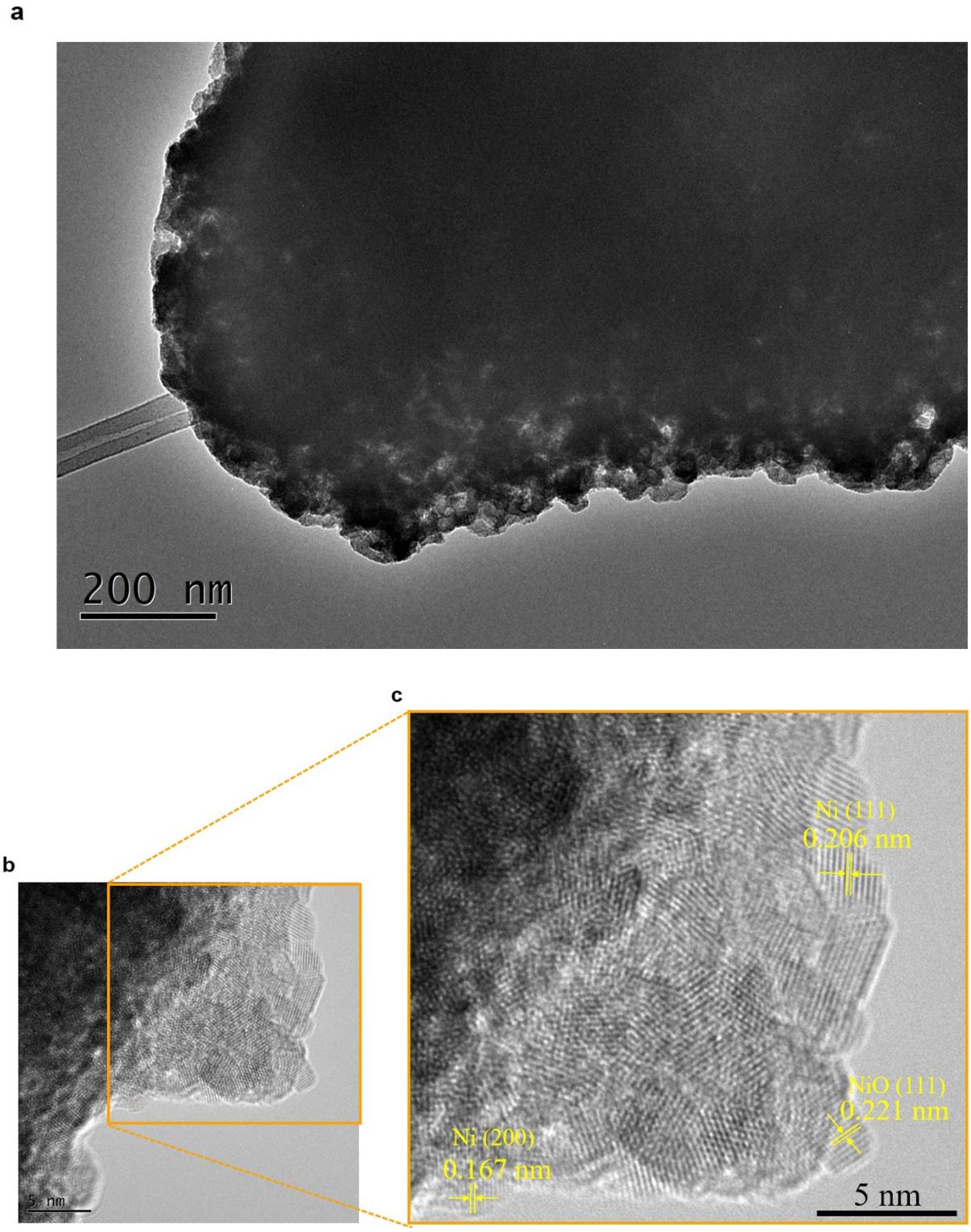

Fig. S3 TEM and HRTEM images of nanoparticles from As synthesized *hp*-Ni showing a) overall structure; b) randomly arranged crystal lattices of Ni and NiO, c) close-up image of (b), showing the d-spacing of 0.206 and 0.167 nm of fcc Ni (111) and (200) planes, respectively. The d-spacing of 0.221 nm corresponds to NiO (111) plane.

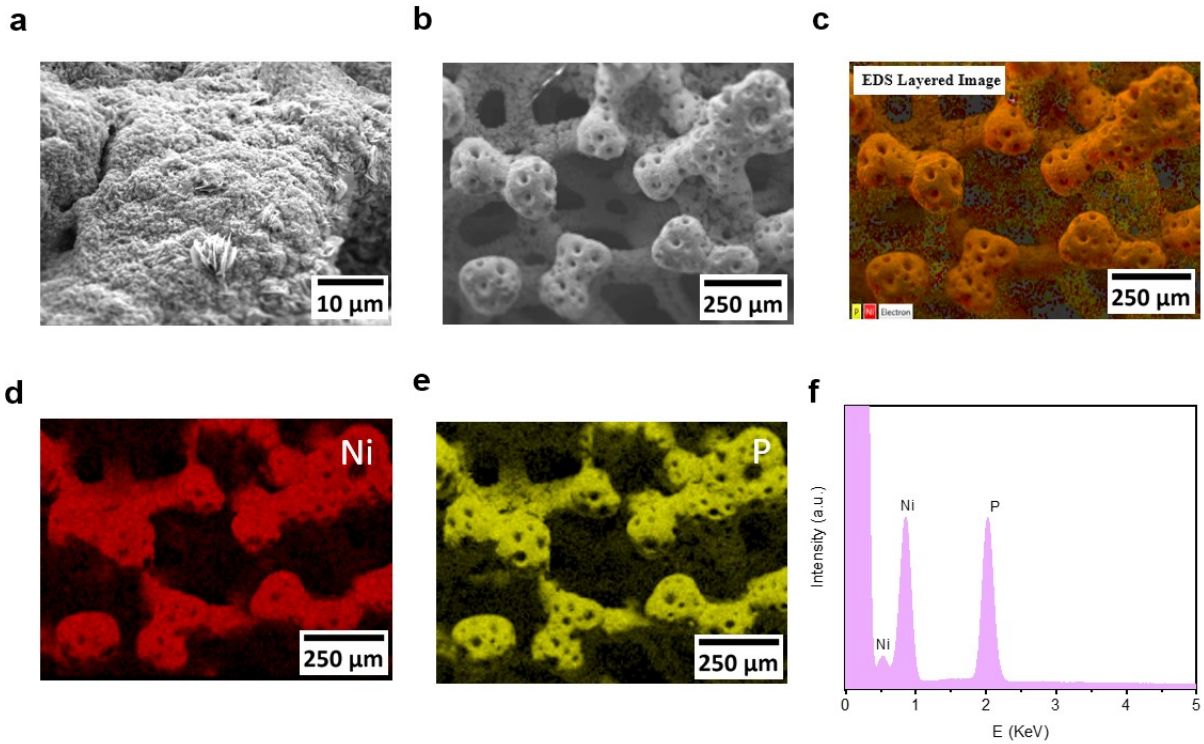

Fig. S4 Ni_2P - a) SEM image of electrocatalyst surface; b) SEM image used for EDS analysis; Ni_2P EDS, c) combined layered image of the detected elements, d) nickel element mapping image, e) Phosphorus element mapping image; f) EDS spectrum of area in image (b)

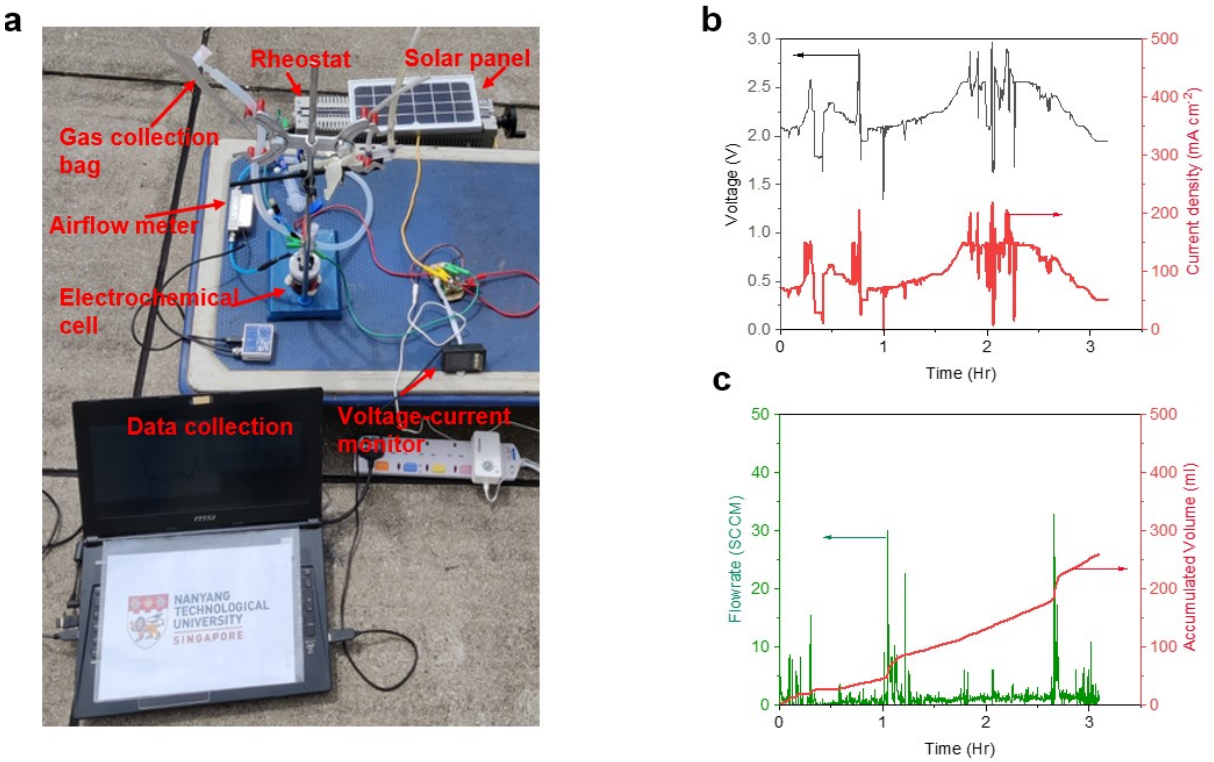

Fig. S5 Solar driven electrooxidation of HPW to Formic acid a) Setup of experiment b) Voltage and current density against time plot c) Gas airflow rate and accumulated volume with time plot

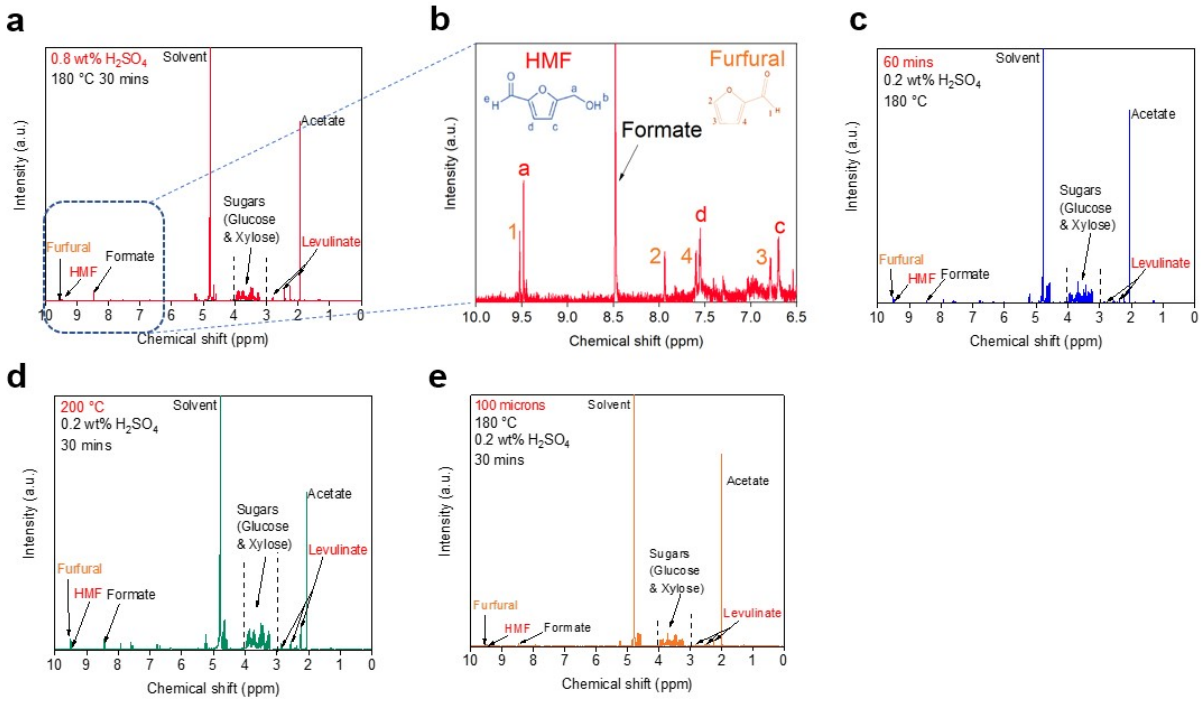

Fig. S6 ^{1}H NMR spectrums of microwave-assisted hydrothermal of Paulownia wood focused on - a) 0.8 wt% H_2SO_4, b) Zoom in of NMR spectra of (a) from 6.5 to 10 ppm with insets of HMF and Furfural compound and their corresponding peak location; c) 60 mins; d) 200 °C; e) 100-micron size.

(Note: for NMR spectrums (c-e), for simplification, HMF is represented only with peak "a" and Furfural is represented only with peak "1". In fact, all peaks a, d, and c of HMF and 1, 2,4 and 3 of Furfural can be represented.)

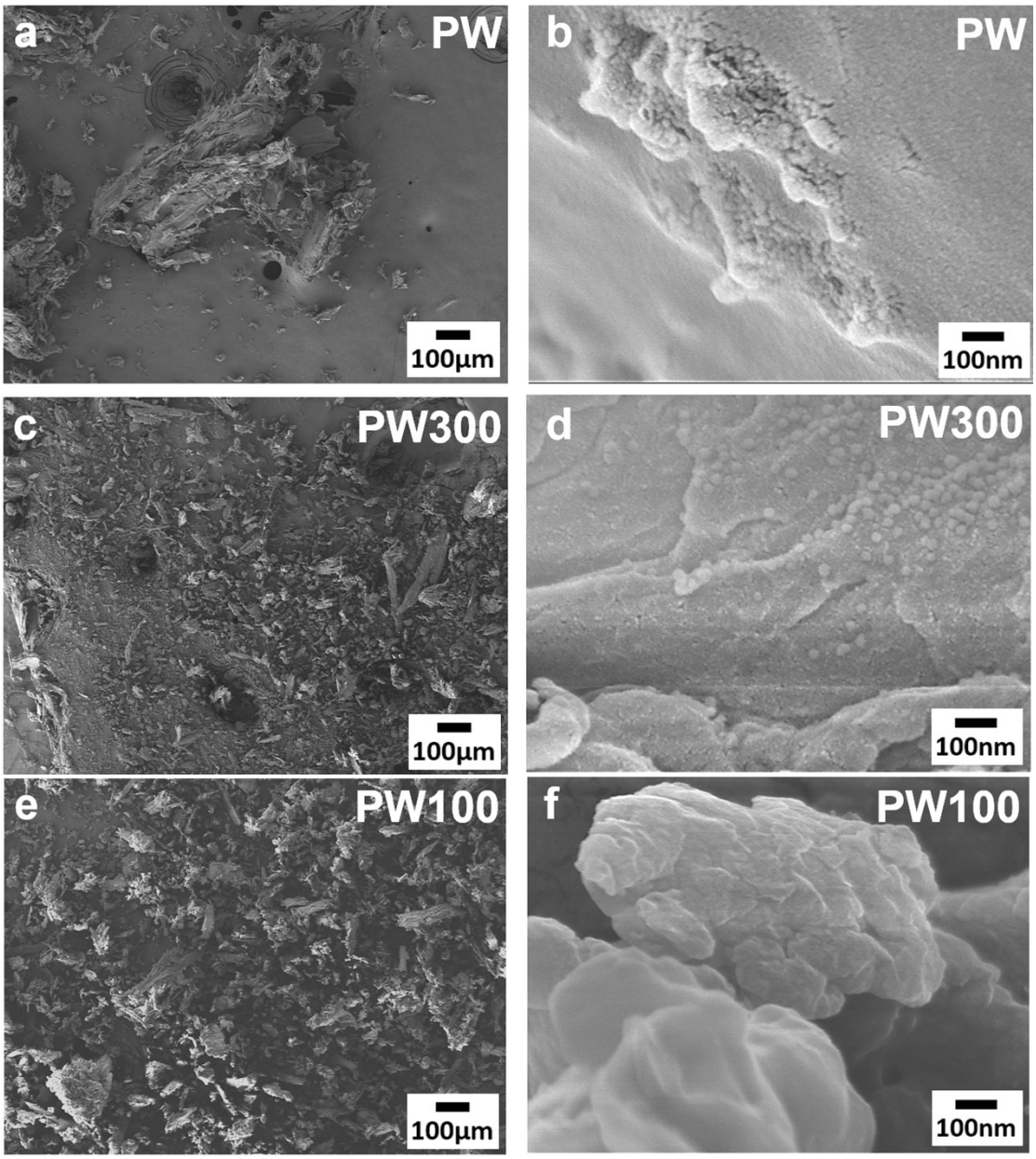

Fig. S7 FE-SEM images of Paulownia wood (PW) before MHT at different magnifications: a) 80 ×, b) 100,000 ×; and Paulownia wood of 300 microns (PW300) at different magnifications: c) 80 ×, d) 100,000 ×; and Paulownia wood of less than 100 microns (PW100) at different magnifications: e) 80 ×, f) 100,000 ×.

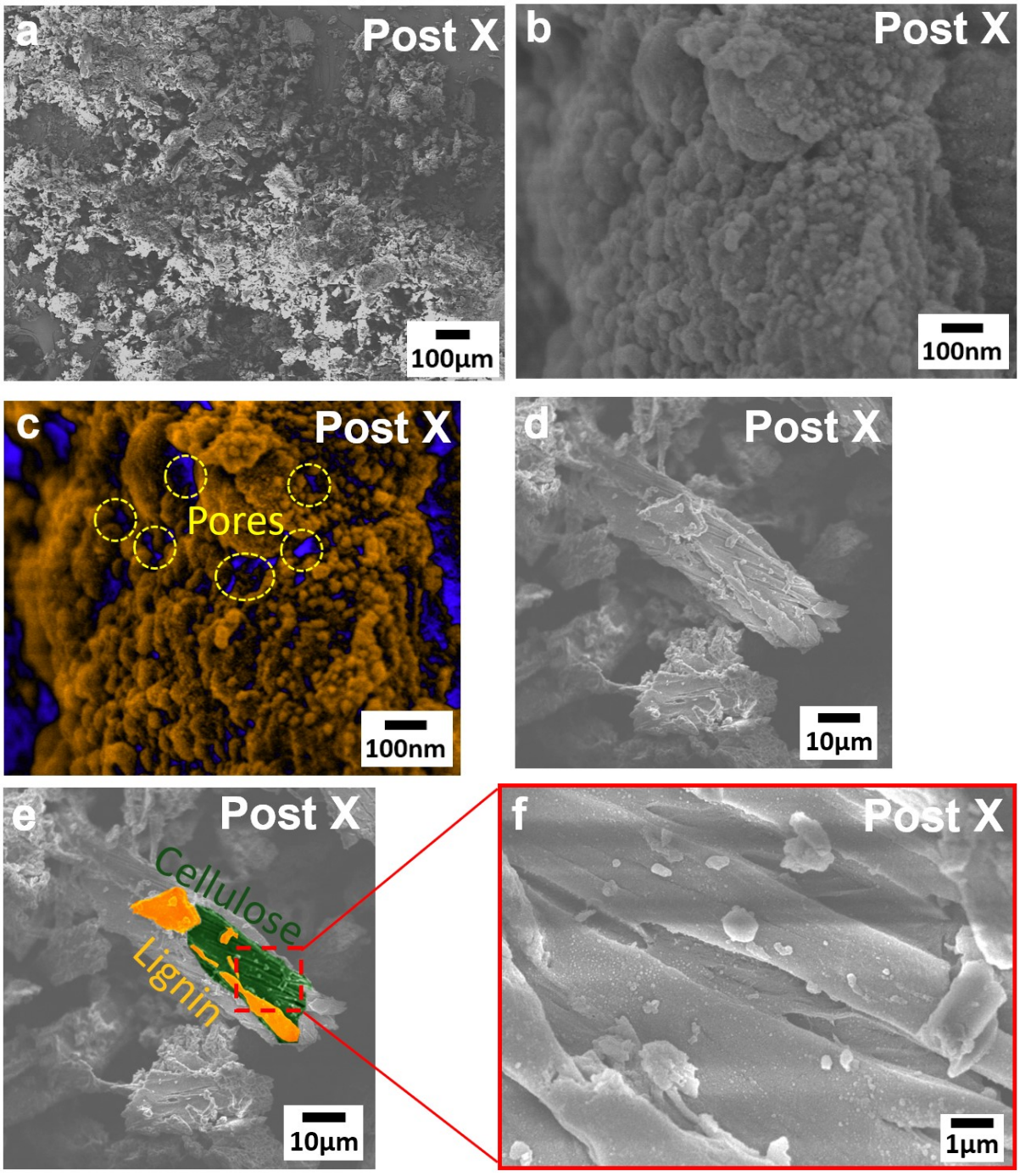

Fig. S8 FE-SEM images of Post xylose extraction (Post X) at different magnifications - a) 80 ×, b) 100,000 ×, c) color-enhanced image of (b) with pores circled in yellow; d) 1000 ×; e) color-enhanced image of (d) with lignin highlighted in orange and cellulose in green, and f) close-up image of (e)

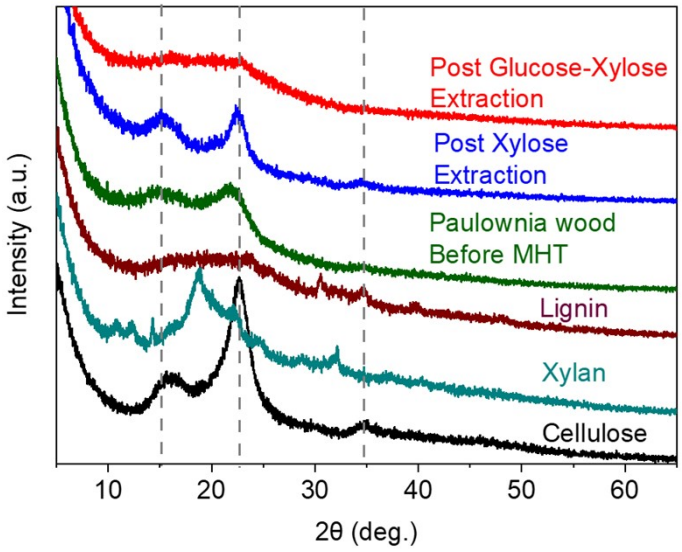

Fig. S9 XRD patterns of reference samples cellulose, hemicellulose (xylan) and lignin in comparison to Paulownia wood samples before and after MHT (Post xylose and glucose-xylose extractions)

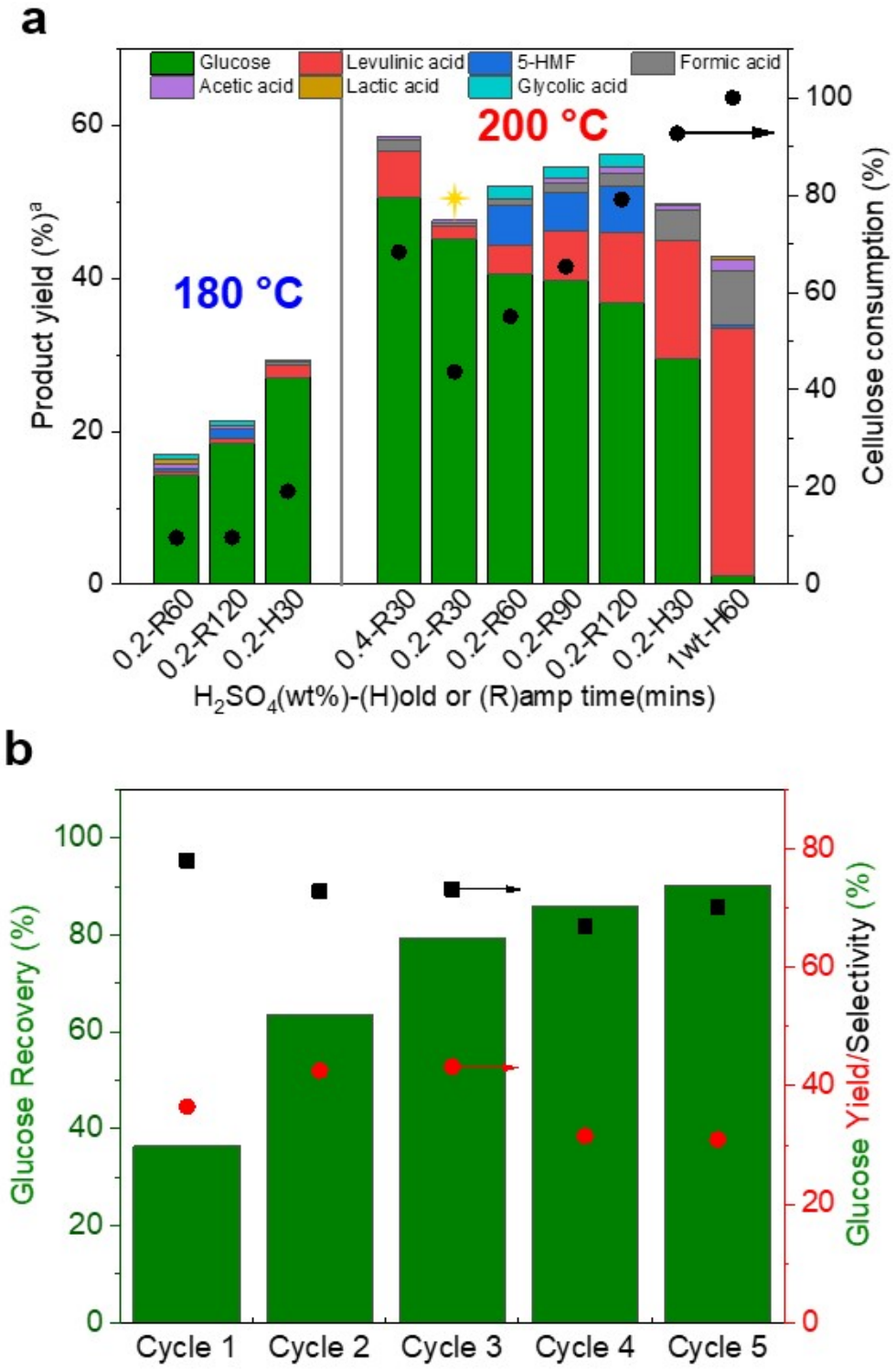

Fig. S10 a) Study of glucose conversion from cellulose residue from optimized MHT - Effect of acid concentration, heating mode and temperature; b) Consecutive cycles of MHT of cellulose residue with glucose recovery and yield based on initial cellulose content in residue, and glucose selectivity was calculated based on measured liquid TOC.

*Yellow star indicates the selected condition for cellulose residue conversion.

[a] Product yield based on moles of carbon from cellulose (residue from after MHT)

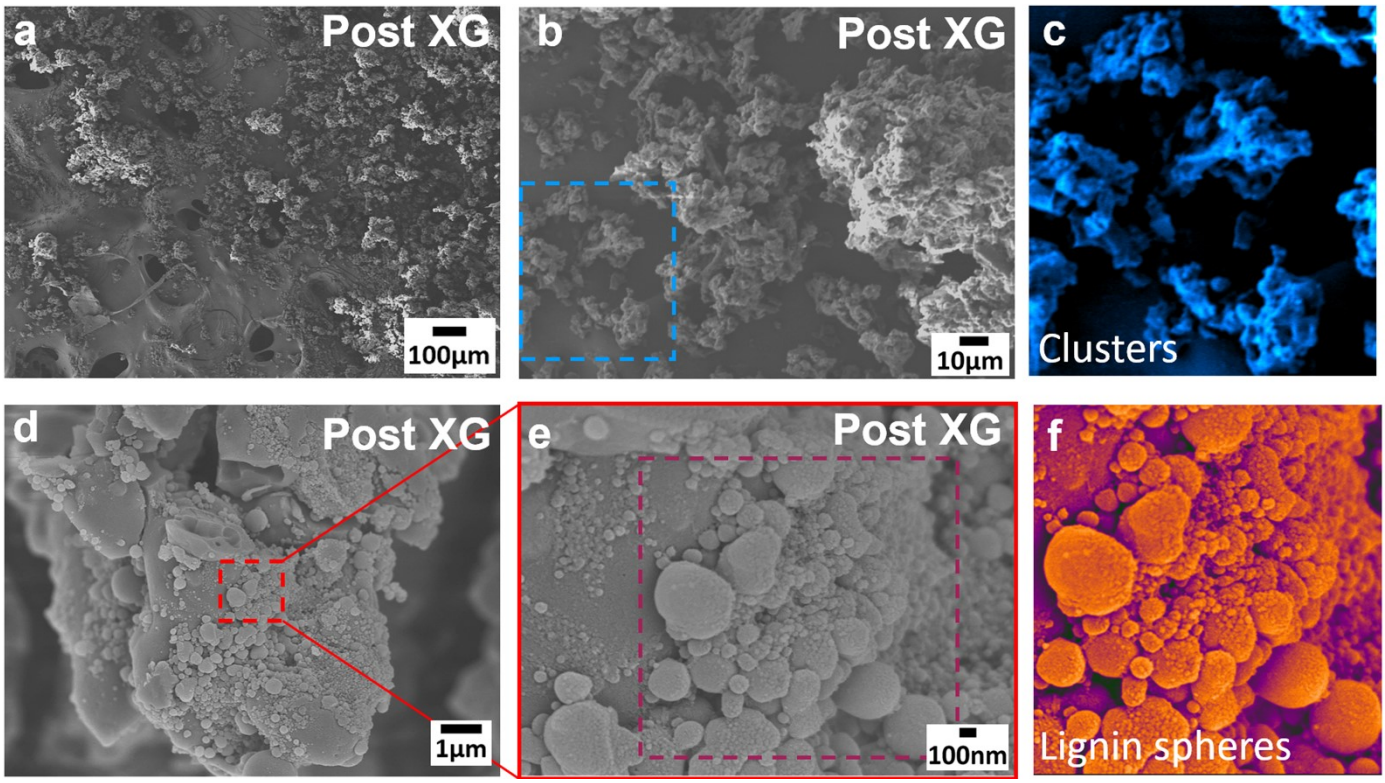

Fig. S11 FE-SEM images of post xylose-glucose extraction (Post XG) at - a) magnification of 80 ×, b) 650 ×. c) color-enhanced image of dotted blue area in image (b) with small, clustered size particles (blue). d) magnification of 10,000 × of surface of cluster and e) close-up image of (d); f) color-enhanced image of dotted purple area in image (e) with lignin nanospheres (orange) with diameters ranging from 5 to 50 nm on lignin agglomeration (purple)

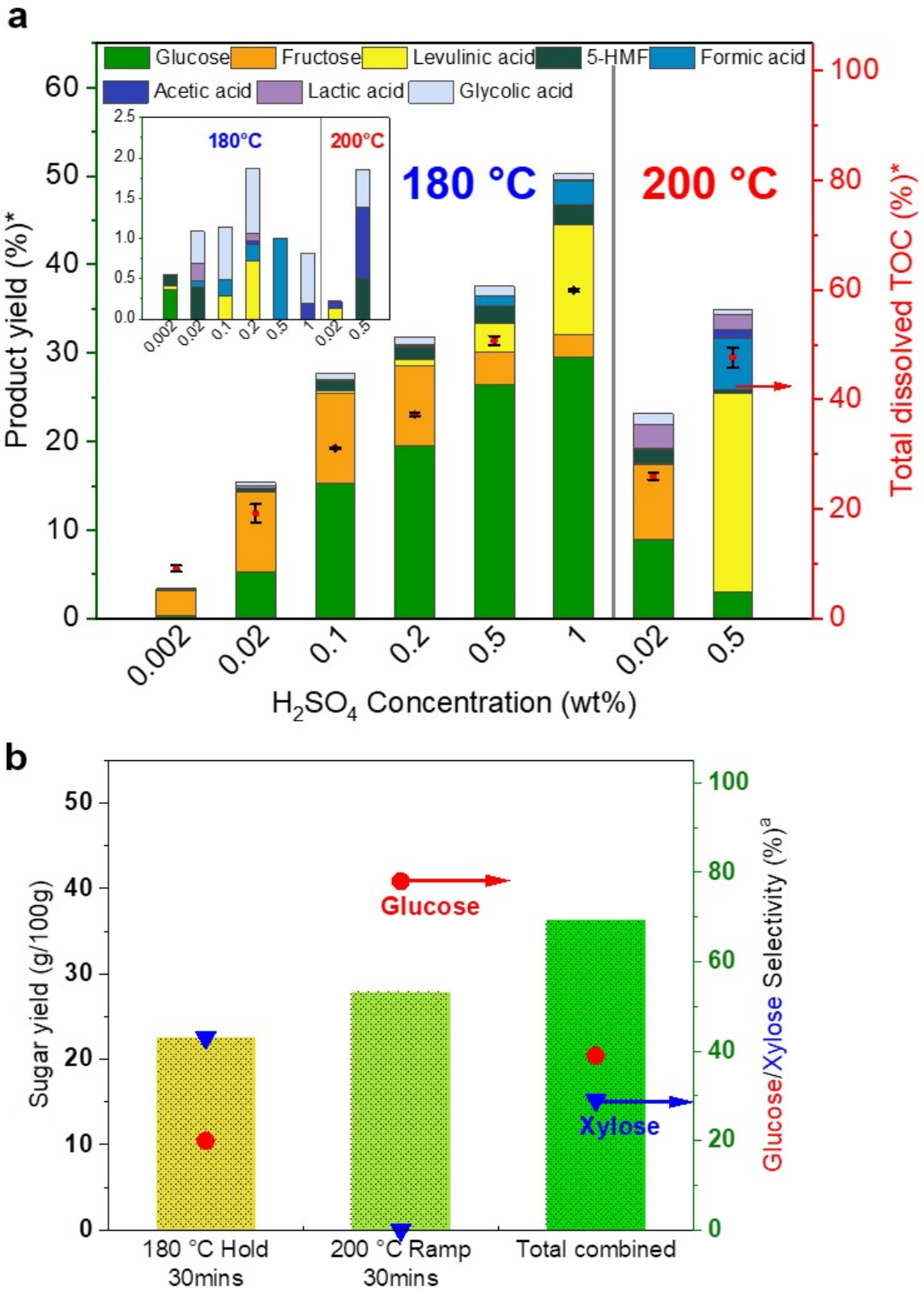

Fig. S12 a) Cellulose control study - Influence of acid concentrations and microwave set temperatures (180 and 200 °C) on product yield and dissolved TOC, Inset: shows the zoom-in of products of less than 1% *calculated based on moles of carbon of initial cellulose; b) Comparison of 180 °C hold 30mins (optimized MHT), 200 °C ramp 30 mins (cellulose-residue conversion) and their total combined sugar yield for paulownia wood MHT with glucose and xylose selectivity.

[a] Product selectivity based on measured liquid TOC.

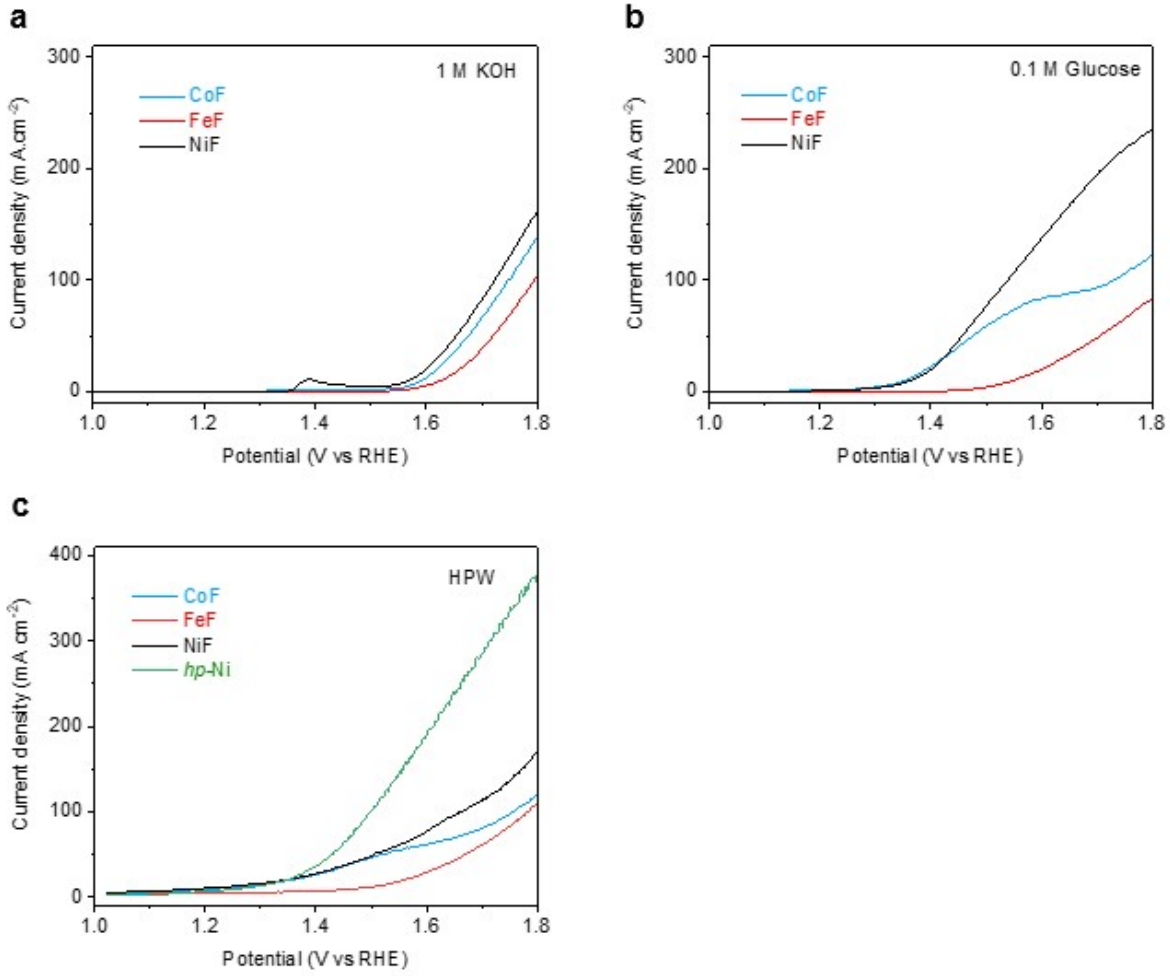

Fig. **S13** Positive sweep LSV with nickel foam (NiF), iron foam (FeF), and cobalt foam (CoF) in a) 1 M KOH; b) 0.1 M Glucose; c) HPW.

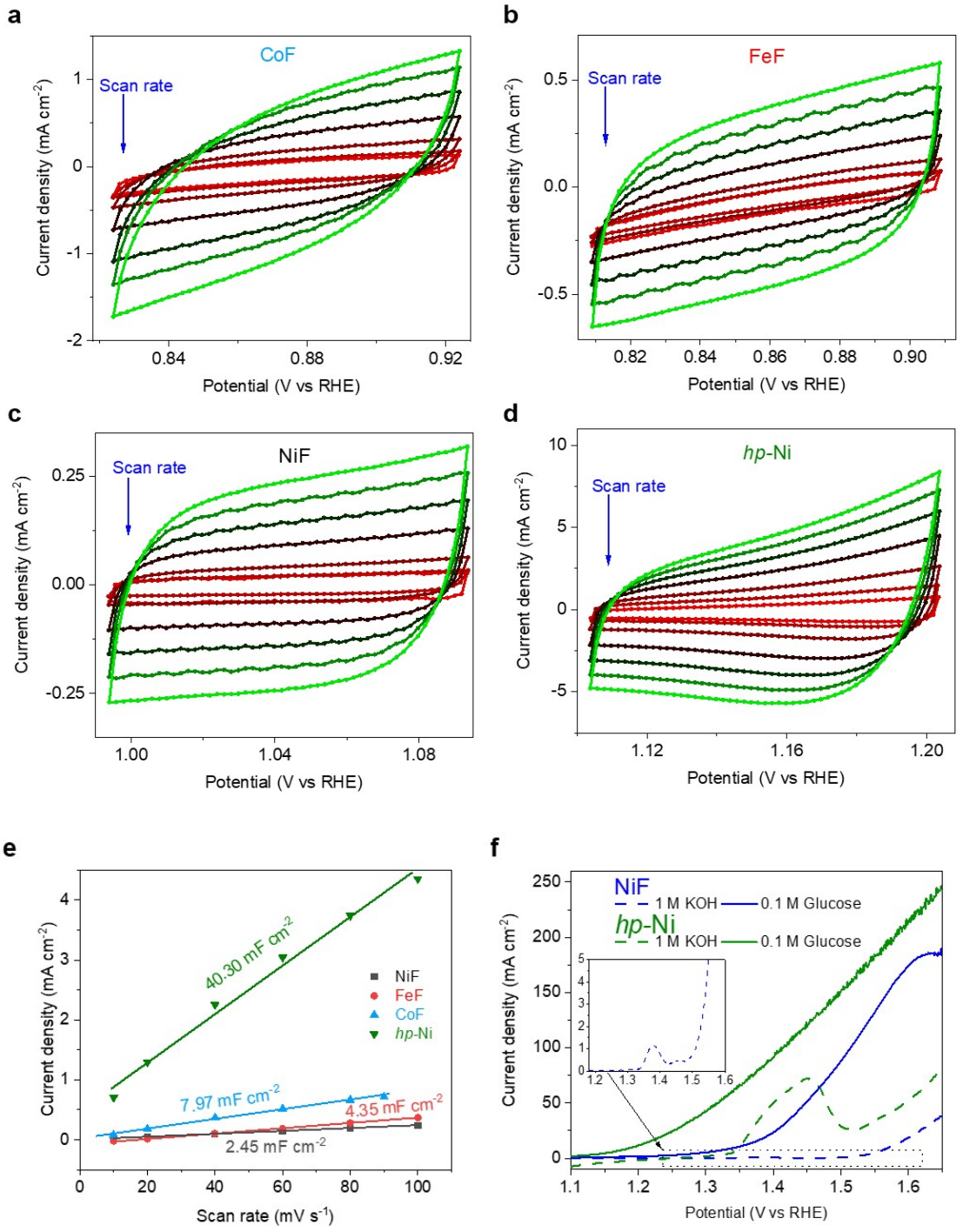

Fig. S14 Electrochemical active surface area (ECSA) measurements. CV curves of - a) CoF, b) FeF, c) NiF, and d) *hp*-Ni collected in 1 M KOH solution at the non-Faradaic region with different scan rates. e) Linear-fitted scan rate dependence of the current density difference at the open circuit potential from CV curves of NiF, FeF, CoF and *hp*-Ni; and f) LSV curves of *hp*-Ni (green) and NiF (blue) as working anode in 1 M KOH solution (dashed lines) and 0.1 M Glucose in 1 M KOH solution (solid lines).

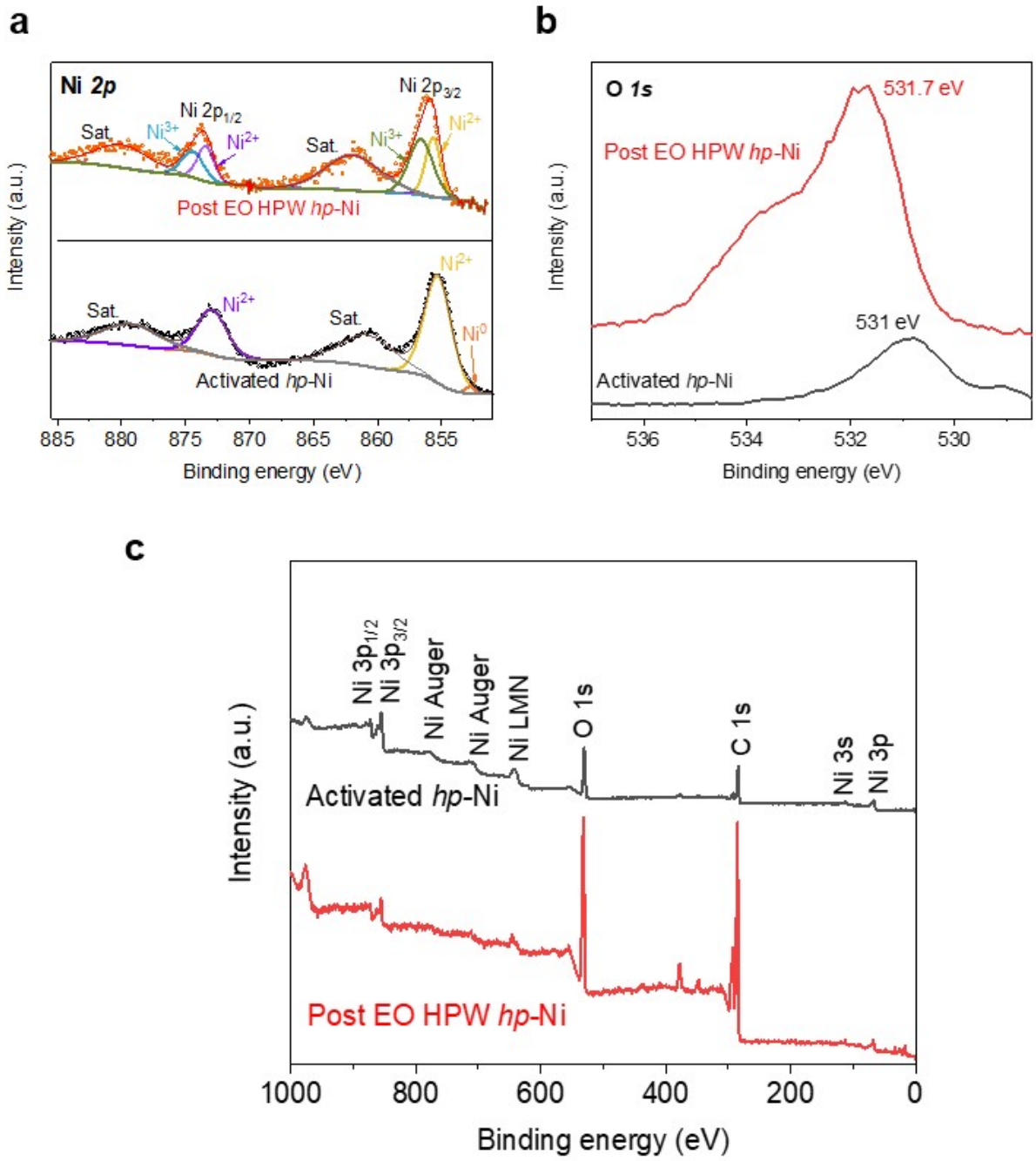

Fig. S15 XPS spectra of a) Ni *2p* states, b) O *1s* state, and c) full survey spectra of *Activated hp*-Ni electrode (black spectra) and *Post EO HPW* for 4 h at 1.58 V vs RHE (red spectra)

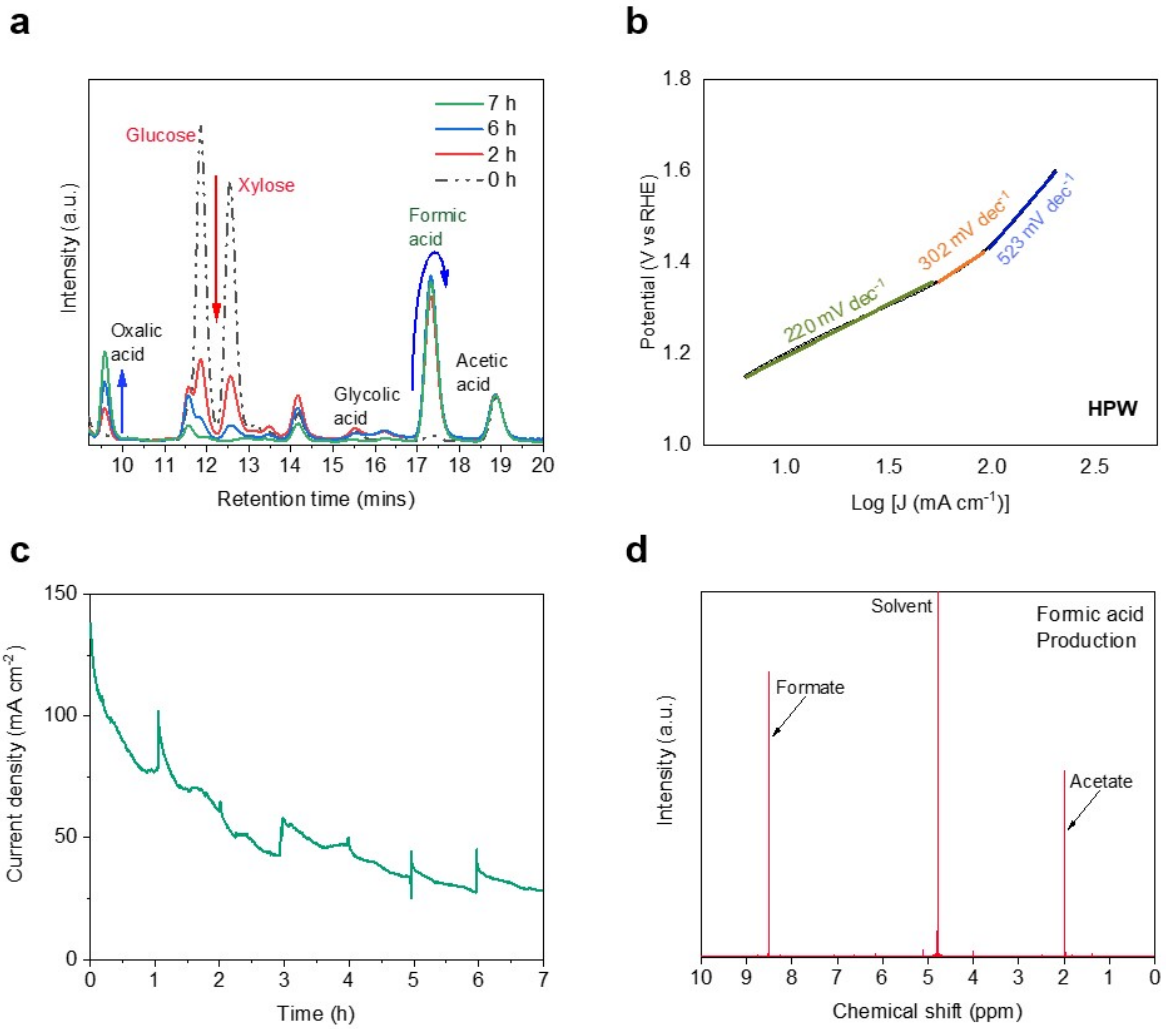

Fig. S16 Formate production from HPW - a) HPLC chromatograms of reactants and products during Formic acid production; b) Tafel plots derived from current–potential curves obtained of *hp*-Ni electrode at scan rate 5 mV s^{-1} in HPW; c) Chronoamperometry at constant potential at 1.58 V vs RHE Product characterization; d) ^{1}H NMR spectrum of pretreated Paulownia wood to formic acid with applied charges 2284 C.

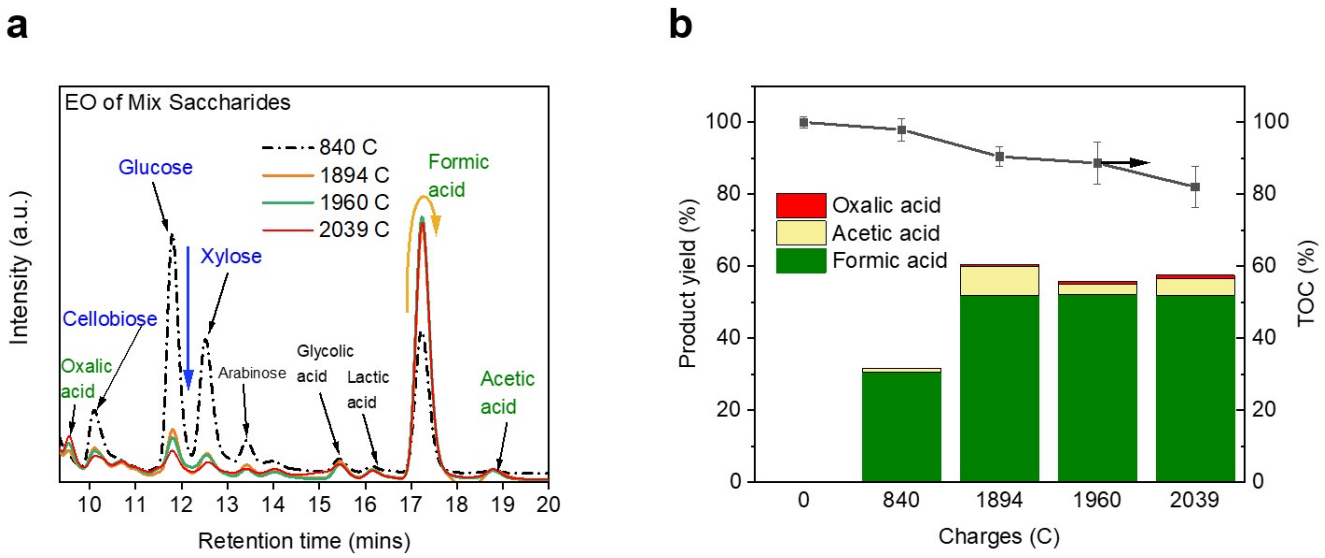

Fig. S17 Electrooxidation of saccharides mixture (carbon mole ratio of 10% cellobiose, 35% xylose and 55% glucose), a) HPLC chromatograms at different intervals at 1.58 V vs RHE and b) Effect of charges on product analysis (oxalic acid, acetic acid and formic acid)

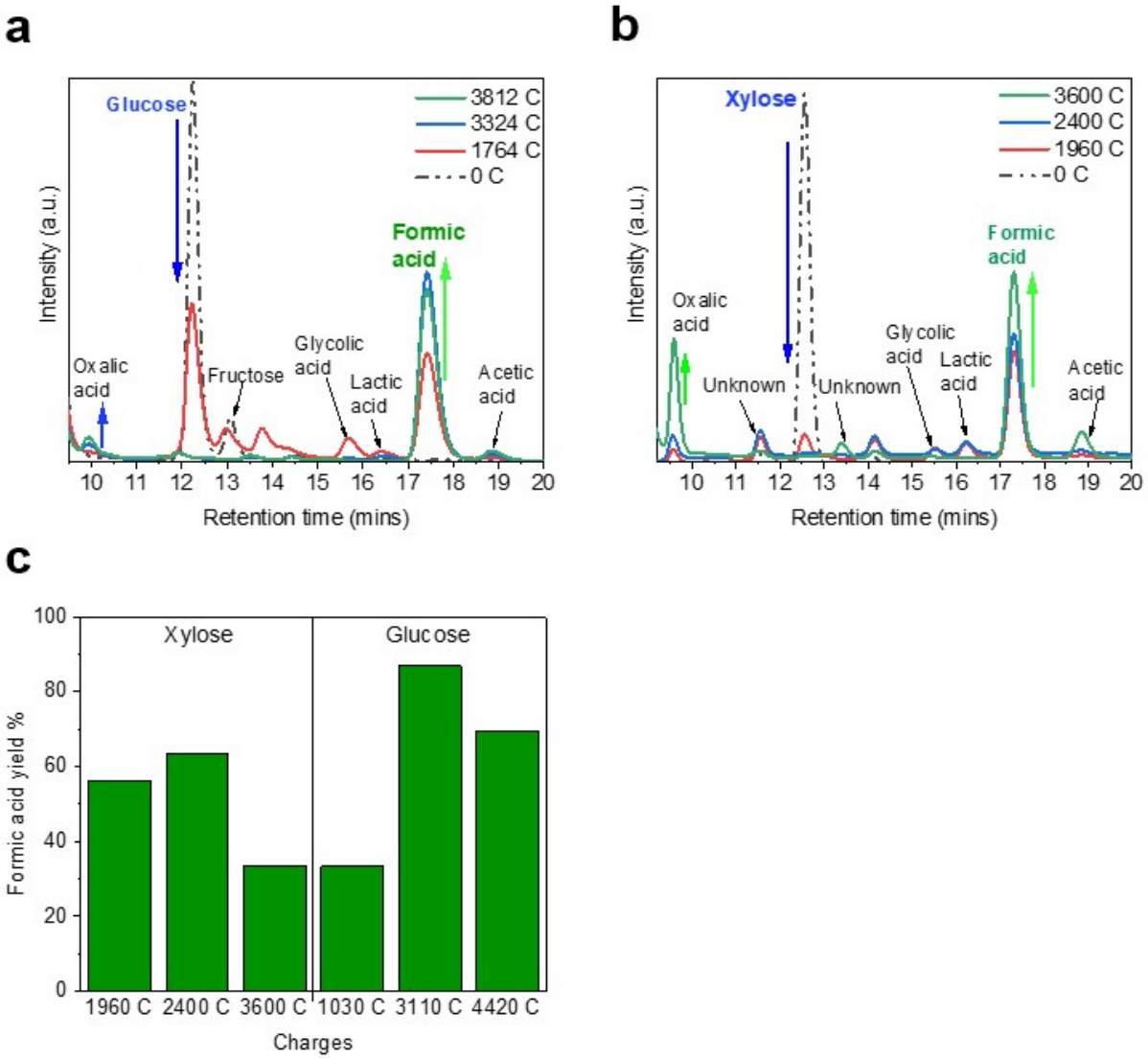

Fig. S18 Monosaccharides electrooxidation to formic acid at 1.58 V vs RHE - a) HPLC chromatograms of glucose electrooxidation to formic acid; b) HPLC chromatograms of xylose electrooxidation to formic acid; c) Effect of charges on formic acid yield % for left (Xylose) and right (Glucose).

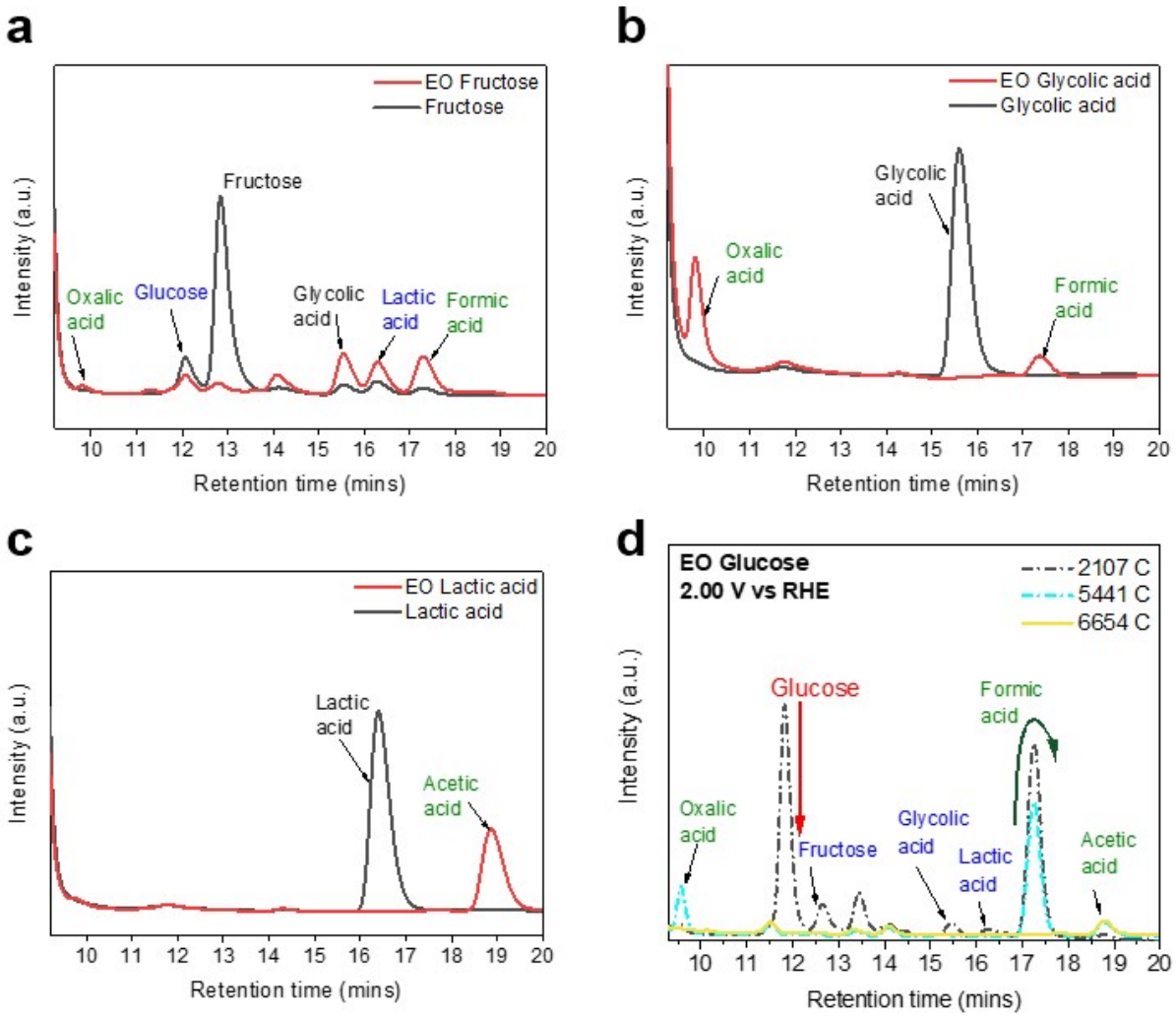

Fig. S19 HPLC chromatograms of electrooxidation of intermediates - a) Fructose; b) Glycolic acid; c) Lactic acid. d) HPLC chromatograms of glucose electrooxidation at 2.00 V vs RHE

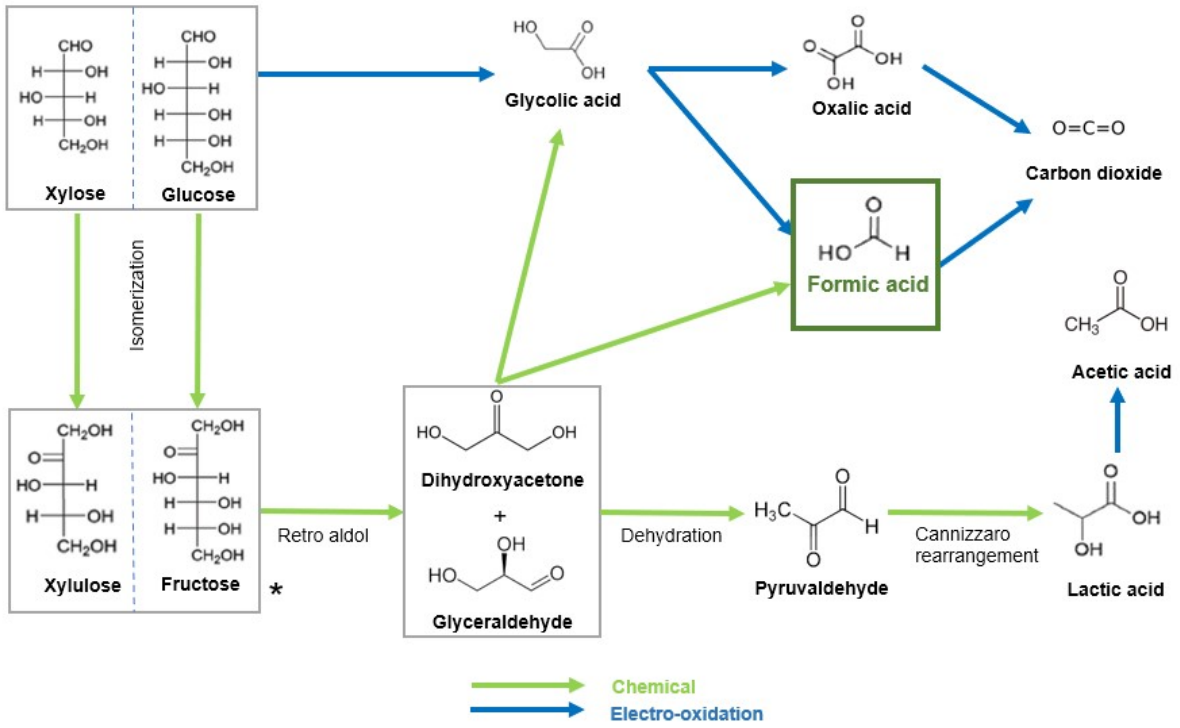

Fig. S20 Proposed reaction pathway of xylose/glucose to Formic acid.

* From xylulose/fructose to lactic acid can be explained by the alkaline isomerization of glucose into enediol, which then forms fructose. Fructose is then transformed into dihydroxyacetone and glyceraldehyde by retro aldol reaction.[1] After dehydrating, pyruvaldehyde is formed, which is re-hydrated to form lactic acid.[2] A further side reaction on the trioses could produce glycolic acid and formic acid. [3] Like glucose, xylose is another aldose sugar type, and it can also undergo the same isomerization reaction to form xylulose.[4]

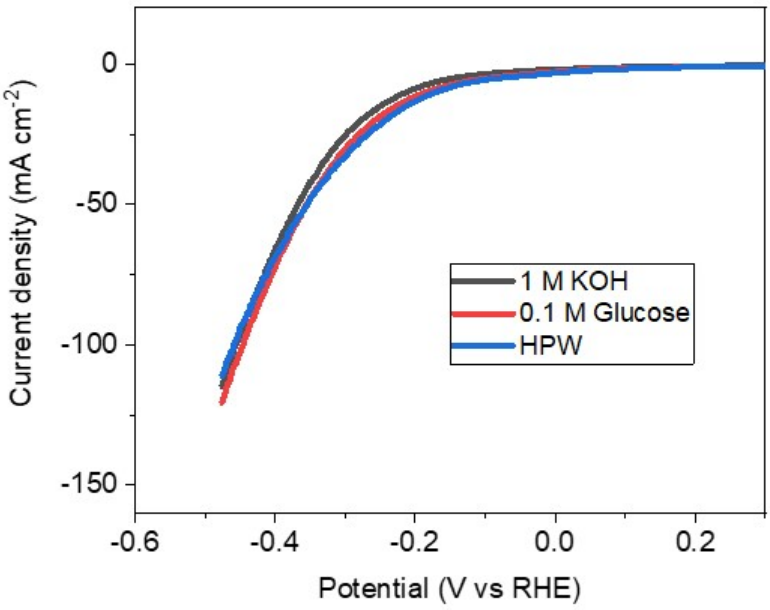

Fig. S21 LSV of Ni_2P cathode anode (black curve: background 1 M KOH, red curve: 0.1 M Glucose in 1 M KOH, and blue curve: HPW)

Table S1

Ball Milling Parameters and Particle Size Distribution for Wood

Parameters	Speed (RPM)	Time (mins)	Energy consumed* (kJ)	Particle size (wt. %) < 100 microns	Particle size (wt. %) 100-300 microns	Particle size (wt. %) > 300 microns
A1	500	15	8.3	19	63	18
A2	500	30	16.5	22	73	5
A3	500	45	24.8	46	51	3
A4	800	45	88.0	76	21	3

*Ball mill energy consumption calculation is detailed in Supplementary Notes 1.

Table S2

Comparison of oven and microwave-assisted hydrothermal method on *Paulownia* wood to yield equivalent sugar yield (Glucose and xylose)

Heating method	Acid use (volume)	Temperature (°C)	Duration (mins)	Glucose yield (%)	Xylose yield (%)	Energy consumption (kWh)
Oven	0.34 wt% 30ml	210	40	16%	93%	0.265*
Microwave	0.20 wt% 15ml	180	30	22%	100%	0.165

*Energy consumption estimated from holding power of oven with 13 mins ramp time and 40 mins hold time.

Supplementary Notes 1

The estimated energy consumption of ball milling is based on the following equations:

$$Energy\ [J] = Power\ [W] * Time\ [s] \quad \text{(S1)}$$

$$Power\ [W] = Torque\ [Nm] * Speed\ [RPM] * \frac{2\pi}{60} \quad \text{(S2)}$$

$$Torque\ (\tau) = Moment\ of\ Inertia\ (I) * Angular\ Acceleration\ (\alpha) \quad \text{(S3)}$$

where I = 0.5*m*$(r)^2$, m and r are the mass and radius of the loaded cylinder jar, respectively.

α = $((\omega f)^2 - (\omega i)^2)$ / 2t, where ωi (initial angular velocity) is 0 and the time interval (t) in seconds is the time for ball mill to reach the constant final speed.

Combining the 3 equations into 1,

$$Energy\ [J] = C1 * Time\ [s] * Speed^3\ [RPM]\ /\ 2t \quad \text{(S4)}$$

where constant C1 is derived to be $0.5\pi^3 mr^2/30^3$.

*The combined mass (Ball mill jar, milling balls and wood sample) and jar radius are 1.33kg and 0.05m, respectively.

* The time (t) for ball mill to reach constant speed of 500RPM and 800RPM is 13s and 15s, respectively.

*Assumptions of no efficiency losses, friction, and from other sources were made for the above calculation.

Based on the equation 4, different ball milling speeds at fixed duration were used to estimate the ball mill energy consumption and were compared in Table S1, together with their respective wood particle size distribution. Notably, parameter *A4* (800 RPM and 45mins) resulted in majority of the wood particles to be less than 100microns while parameter *A2* (500 RPM and 30mins) generated mostly particles size of 100-300 microns. Inevitably, higher energy consumption was required to generate smaller particles size in contrast to the lowest energy requirement (*A1*: 500 RPM and 15mins) which had 18% of larger particle size (>300 microns).

Supplementary Notes 2

The production process of glucose and xylose from Paulownia wood follows the xylose first–glucose second approach. First, mechanical communion of the wood is processed obtain to powder with particle size of 300 μm after sieving. Then, the powder is loaded to a microwave vessel with solid to liquid loading (1:20) with 0.2 wt % H_2SO_4 to extract xylose in the first step of MHT at 160 °C for 30 mins. After centrifuge, the liquid (xylose-rich with ~100% yield) can be separated from the cellulose-rich residue.

Subsequently, the residue is subjected to multiple MHT at 200 °C with ramp duration of 30 mins with the same acid concentration. This results in a glucose hydrolysate (80% to 90% recovery in 3 to 5 steps) with solid lignin remains after centrifuge.

For further purification to obtain high-purity green chemicals, the xylose hydrolysates can undergo additional purification through boric acid carrier liquid-liquid extraction[5-7], while glucose hydrolysates can be refined using membranes[8, 9] or resin systems[10-12].

References

[1] J. M. Macleod and L. R. Schroeder, "Alkaline Degradation of Cellobiose, 3.6-Anhydro-4-O-(β-D-Gluc0pyranosyl)-D-Glucose, 3, 6-Anhydr0-4-0-Methyl-D-Glucose, and D-Glucose1," *Journal of Wood Chemistry and Technology,* vol. 2, no. 2, pp. 187-205, 1982.

[2] J. De Bruijn, A. Kieboom, and H. Van Bekkum, "Alkaline degradation of monosaccharides V: Kinetics of the alkaline isomerization and degradation of monosaccharides," *Recueil des Travaux Chimiques des Pays-Bas,* vol. 106, no. 2, pp. 35-43, 1987.

[3] A. Takagaki, W. Obata, and T. Ishihara, "Oxidative conversion of glucose to formic acid as a renewable hydrogen source using an abundant solid base catalyst," *ChemistryOpen,* vol. 10, no. 10, pp. 954-959, 2021.

[4] C. M. Brands and M. A. van Boekel, "Reactions of monosaccharides during heating of sugar− casein systems: Building of a reaction network model," *Journal of Agricultural and Food Chemistry,* vol. 49, no. 10, pp. 4667-4675, 2001.

[5] G. John Griffin and L. Shu, "Solvent extraction and purification of sugars from hemicellulose hydrolysates using boronic acid carriers," *Journal of Chemical Technology & Biotechnology: International Research in Process, Environmental & Clean Technology,* vol. 79, no. 5, pp. 505-511, 2004.

[6] G. Griffin, "Purification and Concentration of Xylose and Glucose from Neutralized Bagasse Hydrolysates Using 3, 5-Dimethylphenylboronic Acid and Modified Aliquat 336 as Coextractants," *Separation science and technology,* vol. 40, no. 11, pp. 2337-2351, 2005.

[7] L. Ricciardi, W. Verboom, J.-P. Lange, and J. Huskens, "Selective Extraction of Xylose from Acidic Hydrolysate–from Fundamentals to Process," *ACS Sustainable Chemistry & Engineering,* vol. 9, no. 19, pp. 6632-6638, 2021.

[8] S. C. Lee, "Purification of xylose in simulated hemicellulosic hydrolysates using a two-step emulsion liquid membrane process," *Bioresource technology,* vol. 169, pp. 692-699, 2014.

[9] J. Liu *et al.*, "Preparation of boronic acid and carboxyl-modified molecularly imprinted polymer and application in a novel chromatography mediated hollow fiber membrane to selectively extract glucose from cellulose hydrolysis," *Journal of Separation Science,* vol. 45, no. 13, pp. 2415-2428, 2022.

[10] W. A. Farone and J. E. Cuzens, "Method of separating acids and sugars resulting from strong acid hydrolysis," ed: Google Patents, 1996.

[11] Z.-Y. Sun, T. Wang, L. Tan, Y.-Q. Tang, and K. Kida, "Development of a more efficient process for production of fuel ethanol from bamboo," *Bioprocess and Biosystems Engineering,* vol. 38, pp. 1033-1043, 2015.

[12] J. Liu, Y. Qin, P. Li, K. Zhang, Q. Liu, and L. Liu, "Separation of the acid-sugar mixtures by using acid retardation and further concentration of the eluents by using continuous-effect membrane distillation," *Journal of Chemical Technology & Biotechnology,* vol. 91, no. 4, pp. 1105-1112, 2016.